University of Nebraska - Lincoln
DigitalCommons@University of Nebraska - Lincoln

Faculty Publications from Nebraska Center for Materials and Nanoscience

Materials and Nanoscience, Nebraska Center for (NCMN)

2014

Spin density waves in periodically strained graphene nanoribbons

Nabil M. Al-Aqtash
University of Nebraska at Omaha, nabild@hu.edu.jo

Renat F. Sabirianov
University of Nebraska at Omaha, rsabirianov@mail.unomaha.edu

Follow this and additional works at: http://digitalcommons.unl.edu/cmrafacpub

 Part of the Atomic, Molecular and Optical Physics Commons, Condensed Matter Physics Commons, Engineering Physics Commons, and the Other Physics Commons

Al-Aqtash, Nabil M. and Sabirianov, Renat F., "Spin density waves in periodically strained graphene nanoribbons" (2014). *Faculty Publications from Nebraska Center for Materials and Nanoscience*. 110.
http://digitalcommons.unl.edu/cmrafacpub/110

This Article is brought to you for free and open access by the Materials and Nanoscience, Nebraska Center for (NCMN) at DigitalCommons@University of Nebraska - Lincoln. It has been accepted for inclusion in Faculty Publications from Nebraska Center for Materials and Nanoscience by an authorized administrator of DigitalCommons@University of Nebraska - Lincoln.

Nanoscale

PAPER

View Article Online
View Journal | View Issue

Spin density waves in periodically strained graphene nanoribbons

Cite this: *Nanoscale*, 2014, **6**, 4285

Nabil M. Al-Aqtash*[ab] and Renat F. Sabirianov[ab]

Zigzag graphene nanoribbons (ZGNRs) are antiferromagnetic in the ground state with zero net magnetization due to the compensation of contributions from opposite edges. Uniform deformations (both shear and axial) do not produce magnetization due to symmetry restrictions. However, we report the results of first-principles calculations that predict the induction of spin density waves (SDWs) in ZGNRs under non-uniform periodic strain. Using the density functional theory (DFT) method, we show that a sinusoidal magnetization variation along the axis of the ribbon occurs under a sinusoidal transversal shear strain. SDWs appear due to the presence of a strain gradient that induced asymmetry of magnetization on opposite edges of ZGNRs which do not compensate each other. The amplitude of SDWs is estimated at $\sim 0.066\mu_B$ when deformations transverse to the ZGNR axis have a sinusoidal profile with a period of 88.6 Å and an amplitude of 1 Å. Our study suggests that the periodic lattice deformations strongly affect the magnetic structure of ZGNRs in the case of acoustic phonons or mechanical waves.

Received 22nd November 2013
Accepted 31st January 2014

DOI: 10.1039/c3nr06199j

www.rsc.org/nanoscale

1 Introduction

The properties of graphene, the strongest and most flexible as well as stretchable material, can be tuned by mechanical deformations.[1] In principle, by suitable engineering of local strain profiles, all-graphene electronics could be integrated on a single graphene sheet. In other words, the combination of the in-plane stiffness and off-plane flexibility of graphene is extraordinary, and future applications of its mechanical effects will be valuable.

Several mechanical deformations of graphene and graphene nanoribbons (GNRs), such as roughening, bending, folding, buckling, and twisting, are controllably produced in laboratories,[2–5] Periodic deformation occurs in the case of phonon excitations or mechanical waves (intrinsic ripples). These excitations are expected in the graphene-based electronic and spintronic devices.[6] Mechanical deformations naturally appear in ZGNRs. For example, AFM images of the chemically derived ZGNRs deposited on a substrate show substantial bending when nanoribbons are less than 20 nm wide.[7] Young *et al.* by using Raman spectroscopy have shown that the distribution of strains across the graphene monolayer is relatively uniform at levels of applied strain up to 0.6% but it becomes highly nonuniform above this strain.[8] Moreover, there are reports of controlled texturing on graphene nanoribbons and membranes. Bao *et al.* reported the first direct observation and controlled creation of one- and two-dimensional periodic ripples in suspended graphene sheets, using both spontaneously and thermally generated strains.[9] Xu *et al.* demonstrated atomic control of strain in freestanding graphene using a local attractive force created at the STM tip.[10] Moreover, mechanical vibrations in suspended nanoribbons were generated by D. Garcia-Sanchez *et al.* with sinusoidal variation of strains.[11]

The magnetism of graphene has attracted considerable interest. An increase in the difference between the number of removed A and B sites of the graphene bipartite lattice at zig-zag edges induces net magnetic moments and yields ferromagnetism, particularly in nano-size graphene flakes and nanopores.[12] Recently, a clear hysteresis in magnetization reversal curves of ferromagnetic (FM) zig-zag edged graphene was reported.[13] The magnetism was mainly proposed in modified graphene sheets and in GNRs where magnetism comes from the zig-zag termination of the graphene sheet.[14] The ground state of zig-zag terminated GNRs (ZGNRs) is antiferromagnetic (AFM). There are several proposals to stabilize the ferromagnetic (FM) state in ZGNRs by external factors, such as an interface with magnetic materials,[14,15] an application of an external magnetic field[16] or an electric field.[17]

Long spin diffusion length (>2 μm at room temperature) offers an exceptional basis for the development of spintronic devices.[18] Proximity effects were predicted in graphene using magnetic insulators, such as EuO, pointing toward the possible engineering of spin gating.[19] Spin-filtering at interfaces between close-packed surfaces of Ni or Co and graphite or graphene was predicted with ideal spin-injection.[20] However, only a moderate

[a]*Department of Physics, University of Nebraska at Omaha, Omaha, Nebraska 68182-0266, USA. E-mail: nalaqtash@unomaha.edu; Tel: +1 4025543727*

[b]*Nebraska Center for Materials and Nanoscience, University of Nebraska, Lincoln, Nebraska 68588-0111, USA*

This journal is © The Royal Society of Chemistry 2014

(~10%) magnetoresistance (MR) was observed at room temperature in a spin valve where graphene is sandwiched by two FeNi electrodes.[21] Recently, a nearly 100% negative MR was observed at low temperatures, which remained 56% at room temperature.[22] In addition, several theoretical studies have suggested that GNRs could exhibit magneto-electronic properties, with a very large predicted MR.[4,23,24]

Although, the magnetic properties and mechanical properties of graphene systems were investigated in great detail, the mutual effect of mechanical deformations and magnetic properties has not been extensively addressed.

In this study, based on density functional theory (DFT) calculations, we show that a spin density wave is induced in sinusoidally shear-strained ZGNRs. These types of deformations occur in the case of phonon excitations as well as in the case of propagation of mechanical waves. Specifically, this deformation corresponds to a transverse acoustic phonon mode in infinite graphene sheets with in-plane atomic displacements.

2 Model and computational method

We consider the N-ZGNR (N zigzag chains in width) as a periodic supercell consisting of 36 primitive unit cells of total length $L = 88.6$ Å, where $N = 4, 5, \ldots, 12$. The modeling of a sinusoidal strain deformation in nanoribbons is performed by sinusoidal transverse displacement $u_y = A \sin(2\pi x/L)$, where $x = 0 \ldots L$ is the x-axis atomic position and the nanoribbon length $L = 88.6$ Å. The y-coordinate of an atom in the strained ribbon is calculated as $y_i = y_{i0} + u_y$, where y_{i0} is the y-position of atoms in unstrained ZGNRs, amplitude A is varied from 0 to 5 Å. Fig. 1 shows a schematic atomistic model of a sinusoidally shear-strained 4-ZGNR. Although the model does not describe actual phonon excitations in ZGNRs, it captures the origin of spin–lattice interactions. Specifically, it allows direct investigation of the effect of flexure (curvature) on the magnetism of ZGNRs. To study the effects of the edge symmetry and width of N-ZGNRs, we use the 5-, 7-, 9-, 11-ZGNRs and the 4-, 6-, 8-, 10-, 12-ZGNRs to represent asymmetric ZGNRs and symmetric ZGNRs, respectively. Moreover, to investigate the effect of period (L) of the sinusoidal strain, we considered 4-ZGNRs of three period sizes: $L = 88.6$ Å (a supercell consisting of 36 primitive unit cells), 59.07 Å (a supercell consisting of 24 primitive unit cells), and 44.3 Å (a supercell consisting of 18 primitive unit cells).

Our computational approach is based on an *ab initio* pseudopotential method in the framework of density functional theory.[25,26] The geometry relaxations and electronic structures of the nanoribbons are calculated by using the SIESTA package,[27] using numerical atomic orbitals as basis sets and Troullier–Martin type[28] norm-conserving pseudopotentials. Local Spin Density Approximation (LSDA) is used with the exchange-correlation functional in the Ceperley-Alder (CA) form.[29] The self-consistent calculations are performed with a 350 Ry mesh cutoff. A linear combination of numerical atomic orbitals with a double-ξ polarization (DZP) basis set is used. The convergence criteria for energy were selected to be 10^{-5} eV. The conjugate gradient method is used to relax the ionic coordinates until the force on each atom is less than 0.01 eV Å^{-1}.

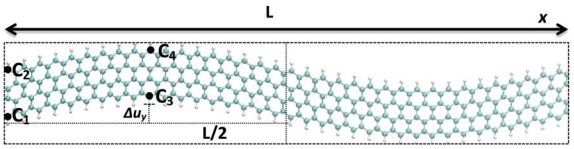

Fig. 1 Atomistic model for zig-zag graphene nanoribbons (4-ZGNRs) with length L under sinusoidal deformation.

3 Results and discussion

We started by performing electronic and ionic relaxation for the planar N-ZGNRs with antiferromagnetic spin configuration to obtain the ground state structures. Then, the nanoribbons were strained by applying a sinusoidally varying shear strain (described by its amplitude A). This deformation corresponds to a transverse acoustic phonon mode in infinite graphene sheets with in-plane atomic displacements. Our system models a frozen phonon with $k = 2\pi/L$. This mode is higher in energy than the ZA acoustic phonon with out-of-plane displacements. However, if out-of plane displacements are suppressed this may become the lowest energy phonon excitation. We performed self-consistent electronic structure calculations for the strained nanoribbons while keeping the atomic positions frozen. Fig. 2(a) shows calculated magnetization induced locally, M, in 4-ZGNRs as a function of the amplitude A at $L = 88.6$, 59.07 and 44.3 Å. We find that the symmetry between the magnetic moment at opposite sides of the ZGNR is lifted and magnetization is induced locally along the nanoribbon. The induced magnetization is calculated as a total magnetic moment for a half-period of the strained ZGNR with the same sign of the in-plane curvature. The induced magnetization increases nearly linearly with the increase of the strain amplitude A of the ribbon until it reaches a saturation value. At higher values of A the induced magnetization is approximately constant. The strain amplitude at which the saturation is reached depends on the period of applied strain L. For $L = 88.6$ Å the saturation occurs at $A = 3$ Å, while the saturation is reached at $A = 2$ Å for the ZGNR of $L = 44.3$ Å. The value of the induced magnetization at saturation increases as a function of period L. This is expected because the induced magnetization depends on the number of edge atoms in the half period. Additionally, the same amplitude of sinusoidal deformation creates a larger strain gradient in the ZGNR with a shorter period of deformation. We plot in Fig. 2(b) the induced magnetization, M, per edge atom as a function of the strain gradient amplitudes, *i.e.* A multiplied by the k-vector (kA). $M(kA)$ for ZGNRs of different periods of deformation collapses into one curve. Clearly, the magnetization per edge atom scales nicely as a function of the strain gradient. Thus, the origin of induced magnetization is due to the presence of a strain gradient.

Fig. 3 shows the induced magnetization as a function of the width of strained asymmetric and symmetric ZGNRs for half (one arc) of the 88.6 Å period with amplitude $A = 1$ Å. At the low values of nanoribbon width ($N = 4$ to 6), we find dependence of

This journal is © The Royal Society of Chemistry 2014

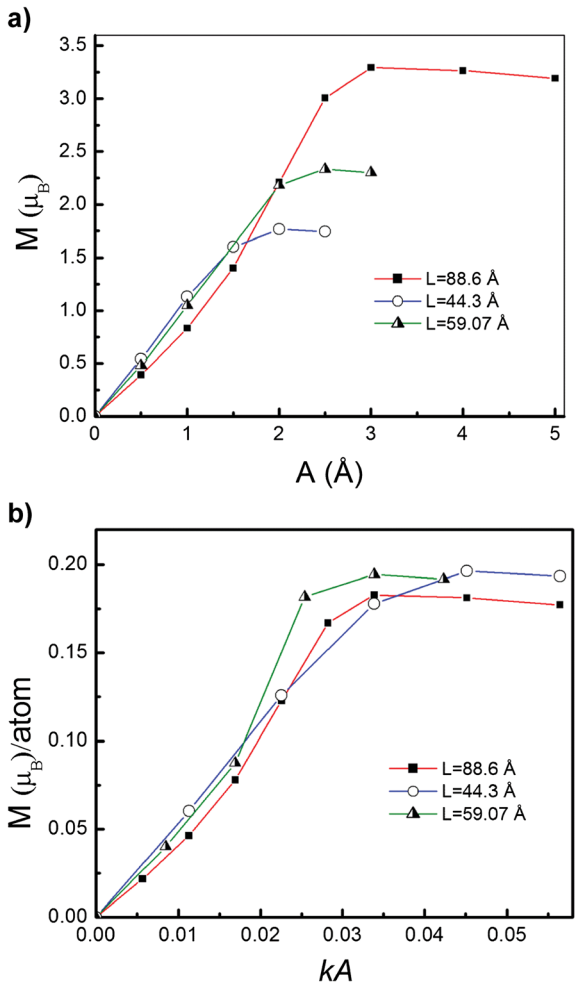

Fig. 2 (a) Induced magnetization, M, defined as the total magnetic moment on the half of the period of shear deformation, *i.e.* $x = 0 \ldots L/2$ in Fig. 1, as a function of the amplitude of shear deformations (A) for three periods of deformation L (88.6, 59.07 and 44.3 Å). (b) Induced magnetization, M, per edge atom as a function of the strain gradient amplitudes, *i.e.* A multiplied by the k-vector (kA).

edge magnetization on the ZGNR thickness. When the width of the ZGNR changes from $N = 4$ to 6 the value of the induced magnetization decreases from about $0.775\mu_B$ to $0.635\mu_B$. However, with increase of the width the edge magnetization of the ribbon saturates very quickly, as we can see from the value of the induced magnetization for widths $N = 6$ to 12. In term of the edge symmetry dependence, there are minor differences between the values of induced magnetization of asymmetric ZGNRs and symmetric ZGNRs, but they are not striking.

The magnetization induced in the ZGNR is due to the change in the local magnetic moments (LMMs) as a function of the edge curvature. LMMs increase at the convex edge (with the positive curvature) and decrease at the concave edge (negative curvature). Fig. 4 shows the LMMs of carbon atoms along half (one arc) of the 88.6 Å period of the strained ZGNR with $A = 1$ Å. Strikingly the LMM dispersed in space just like a spin density wave with overall modulation similar to one of the frozen phonon displacements in real space. Thus, we observe the induction of the spin density wave by phonon-like deformation.

Fig. 5 shows the variation of local magnetic moments along the edges of sinusoidally strained ZGNRs with $L = 88.6$ Å as well as magnetization as a function of the positions of the carbon atom along the edge of the 4-ZGNR x-axis. The latter is calculated as the sum of the local magnetic moments on opposite edges. Clearly there is a correlation between mechanical deformations and the induced spin density wave (SDW), with nodes of spin density waves occurring when opposite edges have the same zero local curvature. Here, we define the spin density wave (SDW) as a periodic modulation of electron spin density where the period of modulation is different from the one of the ions in the ideal lattice. The maximum of SDWs occur at positions with the largest difference in the curvature of opposite edges. The fitting of SDWs to the sin function shows nearly perfect match. Thus, the SDW has the same spatial characteristics as the underlying deformation causing its appearance. The amplitude of the SDW is estimated at $\sim 0.066\mu_B$ for sinusoidal deformation (of amplitude $A = 1$ Å).

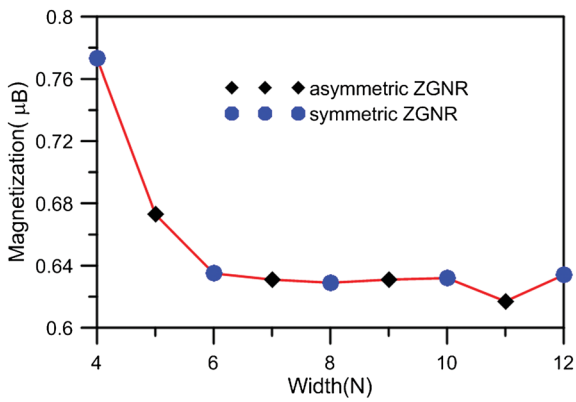

Fig. 3 Induced magnetization as a function of the width (N) of strained asymmetric and symmetric ZGNRs for half (one arc) of the 88.6 Å period with amplitude $A = 1$ Å.

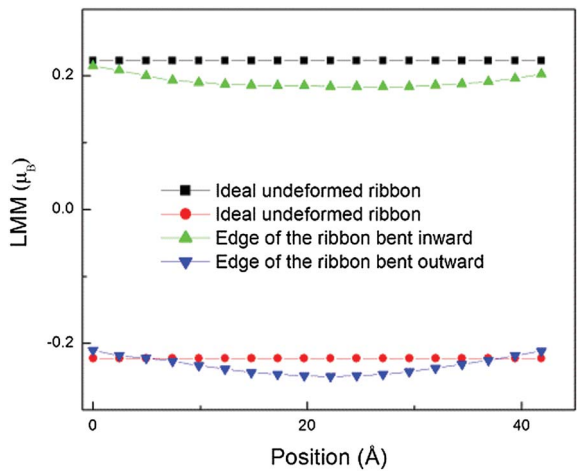

Fig. 4 Local magnetic moments as a function of the x-position of the carbon atom along the edge of 4-ZGNRs for the undeformed nanoribbon and the one sinusoidally strained with $L = 88.6$ Å and $A = 1$ Å.

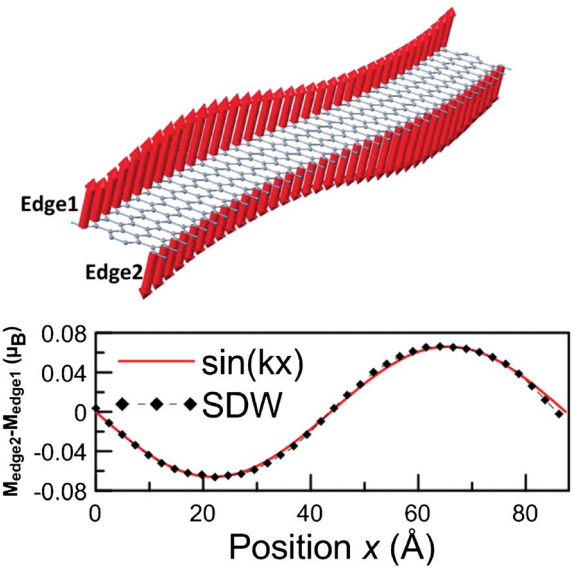

Fig. 5 (Top panel) local magnetic moments (LMMs) along the edges of sinusoidally strained 4-ZGNRs. (Bottom panel) spin density wave along the axis of ZGNRs.

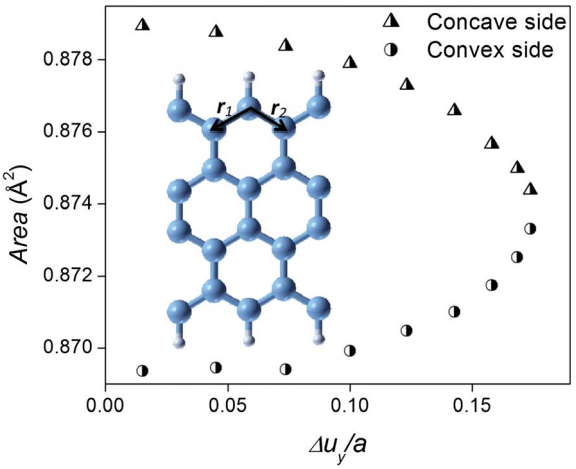

Fig. 6 The edge area "area" of sinusoidally strained (circles: convex edge, triangles: concave edge) 4-ZGNRs as a function of shear strain ($\Delta u_y/a$).

This SDW amplitude is 1/3 of the local magnetic moments at the ZGNR edges ($\sim 0.2\mu_B$). Thus, spin–lattice coupling in graphene is very strong.

Typically, the spin–phonon coupling is relatively weak, but we find that in graphene this coupling is significant. This result is valid in Born-Oppenheimer approximation (ABO) because the frozen phonon-like deformation was used to model this coupling assuming that the electronic structure adjusts fast compared to slow phonon movements. The validity of ABO in application to graphene has been discussed recently and our result could provide an alternative way to explore this issue.[30]

Sinusoidal strain causes very small charge transfer at the edge atoms (less than $0.005e$ per site calculated per atomic sphere). Surprisingly, there is almost no charge transfer for sites of largest curvature. Thus, charge transfer is unlikely the cause of SDWs.

The induced SDW originates from the response of the local magnetic moments at two edges of ZGNRs to the strain, specifically, the non-uniform one. Although formally the in-plane shear stress is the same at opposite edges of the ZGNR, due to the termination, the edge stress is quite different at two opposing edges due to the curvature of edges. We introduce the area covered by radial from a carbon edge atom to two nearest carbon atoms as a measure of the local strain. We defined this area as the edge area "area", which is calculated as:

$$\text{Area} = \frac{1}{2}\vec{r}_1 \times \vec{r}_2$$

where $\boldsymbol{r}_1$ and $\boldsymbol{r}_2$ are vectors connecting the carbon atom at the edge to its nearest neighbors, as shown in Fig. 6. Because this area is connected to the bond angle in the carbon edge "chain", the increase/decrease of the edge area measures local deformations including not only the bond length change but also the concavity. The connection between the shear strain and the "area" parameter is shown in Fig. 6. The shear strain is defined as $\Delta u_y/a$, where $\Delta u_y = u_y(x + \Delta x) - u_y(x)$ is a deformation along the y-axis occurring between two points separated by Δx, and $a = 2.42$ Å is a lattice constant of the graphene unit cell. Clearly, the edges of opposite concavity have opposite trends with the increase of shear strain. *i.e.* this parameter is instrumental in distinguishing the edges of different curvature.

In Fig. 7 we superimposed the LMM variation as a function of the "area" parameter. The spin-density follows the sinusoidal distortions with the periodic modulations of local magnetic moments. To clarify the origin of spin–lattice interactions we studied the response of ZGNRs to uniform deformations, *i.e.* tensile/compressive strains along the axis of the ribbon. We find that the uniform tensile strain causes the magnetization of the edge to increase nearly linearly with tensile strain, while compressive strain results in its near linear decrease as shown in Fig. 6.

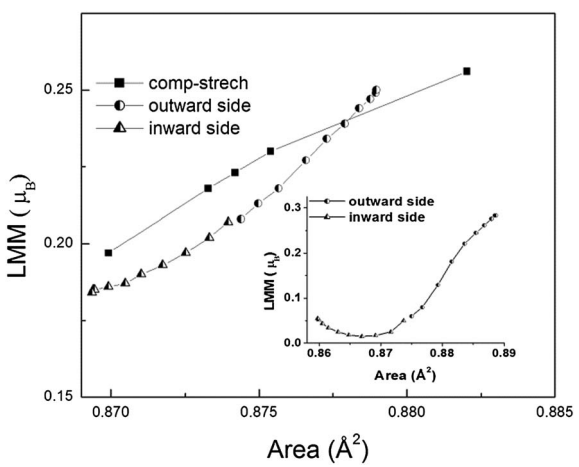

Fig. 7 Local magnetic moments (LMMs) as a function of the edge area of uniformly (black squares) and sinusoidally strained (circles: convex edge, triangles: concave edge) 4-ZGNRs with $L = 88.6$ Å. Main graph is for amplitude $A = 1$ Å, inset is for $A = 3$ Å.

This journal is © The Royal Society of Chemistry 2014

Clearly, there is an overall correlation between the results of uniform and non-uniform strain. However, this correspondence is far from being very close. There are obviously different slopes of $M(A)$ for deformations at the opposite edges in the case of sinusoidal deformations. Also, there is a noticeable non-linearity of $M(A)$. When the amplitude of sinusoidal distortions increases, the deviations from the dependence between LMMs and area become strongly nonlinear.

There is a drastic difference in the effect made by distortions on the electronic states in ZGNRs in the case of uniform and non-uniform strains. The band structure in the case of uniform compressive and tensile strains shows a change in the dispersion of bands as shown in Fig. 8. As we can see from the figure, the bands become more dispersed under compressive strain. Particularly, the energy of bands close to Fermi energy (E_F) at the X point does not change significantly under uniform strain while at the Γ point the eigenvalues move further away, *i.e.* gets lower below E_F and higher above E_F. However, in addition to the change in dispersion, bands of ZGNRs with sinusoidal non-uniform strain show an appearance of localized states which manifest itself as flat bands across the Brillouin zone separated on the energy scale from dispersed bands. Fig. 9 shows a clear representation of this effect in E_K for 4-ZGNRs at $L = 88.6$ Å and $A = 1$ Å.

The magnetization of unstrained ZGNRs is zero due to the antiferromagnetic coupling of the opposite edges. The presence of the sinusoidal strain in ZGNRs does not change total magnetization due to its symmetry. However, locally we may induce an asymmetry between opposite edges due to the difference in its curvatures that results in a local magnetic moment. The origin of this moment induction is due to the difference in the shift of electron states that appear upon non-uniform strain at opposite edges. To illustrate it we plot local densities of states (LDOSs) for atoms at the edges of curvatures with opposite sign and compare them to atoms of near zero curvature, as shown in Fig. 10(a and b) for 4-ZGNRs with $L =$ 88.6 Å. LDOSs were broadened by Gaussian with half-width $\sigma =$ 0.2 in SIESTA calculations to smooth out the sharp peaks of LDOSs due to the localized states. The figure shows that the atoms C_1 and C_2 that are located at the point of near zero curvature (although having a large shear strain) do not have strong asymmetry in LDOSs (Fig. 10a) and give near zero magnetic moment between two of them. In contrast, the atoms C_3 at the concave curvature point and C_4 at the convex curvature point have strong asymmetry in LDOSs with the main peak in majority LDOS for C_4 lying at lower energy than the one of C_3 LDOS (Fig. 10b). It causes the difference in the occupation of states and resulting appearance of uncompensated local magnetic moment because C_4 has larger occupancy in majority LDOS than C_3.

Fig. 10(b–d) also illustrate the variation of LDOS of C_3 and C_4 atoms as a function of magnitude of strain amplitude, in the case of 4-ZGNRs with $L = 88.6$ Å. In unstrained (or uniformly strained) ZGNRs the highest occupied bands have an equal share of states from each edge site, *i.e.* each edge site has the same spin moment. However, with the increase of the amplitude of sinusoidal deformation, the contribution of the state at C_3 to these bands decreases, while LDOS of the C_4 atom increases. At the amplitude $A = 3$ Å the LDOS of the C_3 atom at

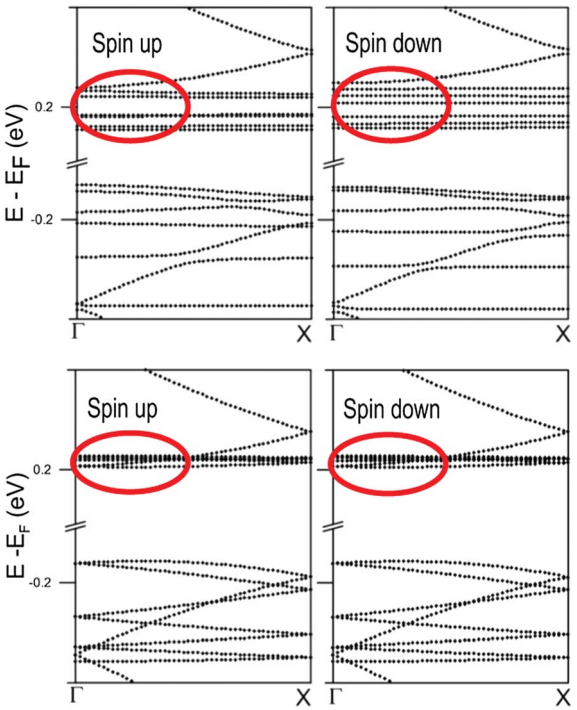

Fig. 9 The band structure of 4-ZGNRs with sinusoidal strain at $A = 1$ Å (upper panel) compared to the band structure of unstrained 4-ZGNRs (lower panel) at $L = 88.6$ Å.

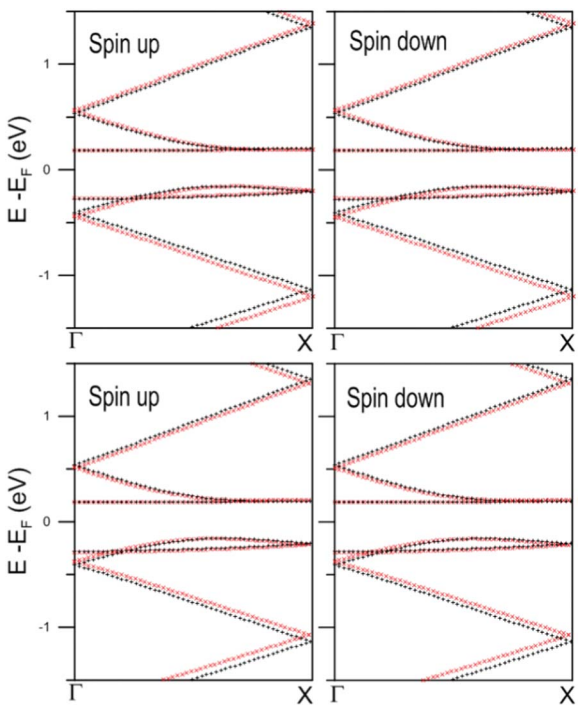

Fig. 8 The band structure of 4-ZGNRs under compressive (1%) (upper panel) and tensile (1%) (lower panel) shown in red (×××) compared to the band structure of unstrained ZGNRs shown in black (+++).

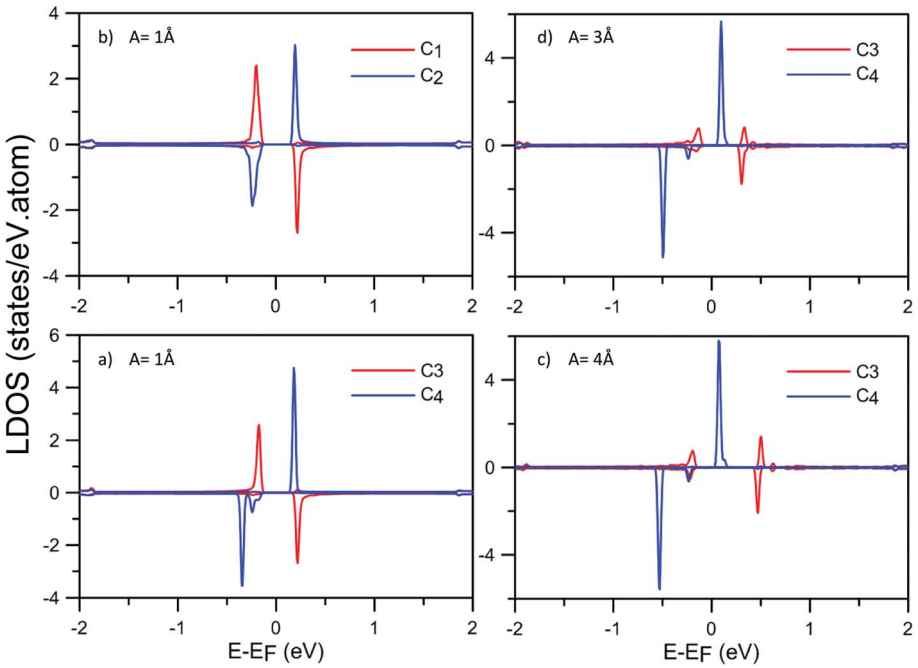

Fig. 10 Local densities of states (LDOSs) calculated for atoms of smallest local curvature (a) and the largest local curvature (b–d) for 4-ZGNRs with sinusoidal strain at $A = 1$, 3, 4 Å at $L = 88.6$ Å. Notations of atoms follow Fig. 1.

the highest occupied bands is very small and cannot reduce substantially with further increase of the amplitude of deformation as can be seen in Fig. 10c and d. At the same time LDOS of C_4 also saturates at $A = 3$ Å (compare Fig. 10c and d). Thus, the magnetization induced by the sinusoidal deformations saturates at $A = 3$ Å and does not increase substantially with further increase of A as can be seen in Fig. 2.

The discussed above edge asymmetry can be used to induce a local magnetic moment in graphene nanoribbons by inducing a curvature as we observe in sinusoidally strained ZGNRs. Periodically strained edges may naturally appear in graphene nanoribbons without hydrogen termination.[4] Particularly, mechanical vibrations in suspended nanoribbons may generate a standing wave in graphene nanoribbons with sinusoidal variation of strains.[11] The local moment can be measured by local probe methods such as sensitive magnetic force microscopy or spin-polarized scanning tunneling microscopy. The coupling between spin (magnon) and lattice (phonon) excitations can also be potentially observed in measurements of respective quasi-particle dispersions.

4 Conclusions

We show that sinusoidal strain deformations induce a spin-density wave along the axis of ZGNRs with induced local magnetic moments modulating sinusoidally as well. While, uniform deformations of ZGNRs (both shear and axial) do not produce magnetization due to symmetry restrictions, the deformations with a gradient of strain (curvature) result in the local breaking of the symmetry and induction of local magnetization. The SDW is induced due to the presence of a strain gradient, the induced magnetization on opposite edges does not compensate each other. We estimate the amplitude of the SDW at $\sim 0.066\mu_B$ that resulted from the bending of ZGNRs with the sinusoidal profile $\delta u_y = A \sin(2\pi x/L)$ with $A = 1$ Å and $L = 88.6$ Å. Our study suggests that the magnetic structure in ZGNRs can be controllably modified using strain engineering.

Acknowledgements

This work was supported by NSF-MRSEC (Grant No. DMR-0820521) and NSF (Grant No. DMR-1310542). The University of Nebraska Holland Computing Center has provided computations resources.

References

1 F. Guinea, M. I. Katsnelson and A. K. Geim, *Nat. Phys.*, 2010, **6**, 30–33.
2 J. C. Meyer, A. K. Geim, M. I. Katsnelson, K. S. Novoselov, T. J. Booth and S. Roth, *Nature*, 2007, **446**, 60–63.
3 Z. H. Ni, T. Yu, Y. H. Lu, Y. Y. Wang, Y. P. Feng and Z. X. Shen, *ACS Nano*, 2008, **2**, 2301–2305.
4 T. W. Chamberlain, J. Biskupek, G. A. Rance, A. Chuvilin, T. J. Alexander, E. Bichoutskaia, U. Kaiser and A. N. Khlobystov, *ACS Nano*, 2012, **6**, 3943–3953.
5 L. Elías, A. R. Botello-Méndez, D. Meneses-Rodríguez, V. J. González, D. Ramírez-González, L. Ci, E. Muñoz-Sandoval, P. M. Ajayan, H. Terrones and M. Terrones, *Nano Lett.*, 2010, **10**, 366–372.

This journal is © The Royal Society of Chemistry 2014

6 Y. Zhang, V. W. Brar, F. Wang, C. Girit, Y. Yayon, M. Panlasigui, A. Zettl and M. F. Crommie, *Nat. Phys.*, 2008, **4**, 627–630.
7 X. Li, X. Wang, L. Zhang, S. Lee and H. Dai, *Science*, 2008, **319**, 1229–1232.
8 R. J. Young, L. Gong, I. A. Kinloch, I. Riaz, R. Jalil and K. S. Novoselov, *ACS Nano*, 2011, **5**, 3079–3084.
9 W. Bao, F. Miao, Z. Chen, H. Zhang, W. Jang, C. Dames and C. N. Lau, *Nat. Nanotechnol.*, 2009, **4**, 562–566.
10 P. Xu, Y. Yang, S. D. Barber, M. L. Ackerman, J. K. Schoelz, D. Qi, I. A. Kornev, L. Dong, L. Bellaiche, S. Barraza-Lopez and P. M. Thibado, *Phys. Rev. B: Condens. Matter Mater. Phys.*, 2012, **85**, 121406.
11 D. Garcia-Sanchez, A. M. van der Zande, A. San Paulo, B. Lassagne, P. L. McEuen and A. Bachtold, *Nano Lett.*, 2008, **8**, 1399–1403.
12 E. H. Lieb, *Phys. Rev. Lett.*, 1989, **62**, 1201–1204.
13 K. Tada, J. Haruyama, H. X. Yang, M. Chshiev, T. Matsui and H. Fukuyama, *Phys. Rev. Lett.*, 2011, **107**, 217203–217206.
14 M. Fujita, K. Wakabayashi, K. Nakada and K. Kusakabe, *J. Phys. Soc. Jpn.*, 1996, **65**, 1920–1923.
15 Y. Cho, Y. C. Choi and K. S. Kim, *J. Phys. Chem. C*, 2011, **115**, 6019–6023.
16 W. Y. Kim and K. S. Kim, *Nat. Nanotechnol.*, 2008, **3**, 408–412.
17 Y.-W. Son, M. L. Cohen and S. G. Louie, *Nature*, 2006, **444**, 347–349.
18 N. Tombros, C. Jozsa, M. Popinciuc, H. T. Jonkman and B. J. van Wees, *Nature*, 2007, **448**, 571–574.
19 H. X. Yang, A. Hallal, D. Terrade, X. Waintal, S. Roche and M. Chshiev, *Phys. Rev. Lett.*, 2013, **110**, 046603–046607.
20 V. M. Karpan, P. A. Khomyakov, A. A. Starikov, G. Giovannetti, M. Zwierzycki, M. Talanana, G. Brocks, J. van den Brink and P. J. Kelly, *Phys. Rev. B: Condens. Matter Mater. Phys.*, 2008, **78**, 195419–195429.
21 E. W. Hill, A. K. Geim, K. Novoselov, F. Schedin and P. Blake, *IEEE Trans. Magn.*, 2006, **42**, 2694–2696.
22 J. Bai, R. Cheng, F. Xiu, L. Liao, M. Wang, A. Shailos, K. L. Wang, Y. Huang and X. Duan, *Nat. Nanotechnol.*, 2010, **5**, 655–659.
23 F. Munoz-Rojas, J. Fernandez-Rossier and J. J. Palacios, *Phys. Rev. Lett.*, 2009, **102**, 136810–136813.
24 N. Al-Aqtash, H. Li, L. Wang, W. N. Mei and R. F. Sabirianov, *Carbon*, 2013, **51**, 102–109.
25 P. Hohenberg and W. Kohn, *Phys. Rev.*, 1964, **136**, B864–B871.
26 W. Kohn and L. J. Sham, *Phys. Rev.*, 1965, **140**, A1133–A1138.
27 J. M. Soler, E. Artacho, J. D. Gale, A. Garcia, J. Junquera, P. Ordejon and D. Sánchez-Portal, *J. Phys.: Condens. Matter*, 2002, **14**, 2745–2779.
28 N. Troullier and J. L. Martins, *Solid State Commun.*, 1990, **74**, 613–616.
29 J. P. Perdew and A. Zunger, *Phys. Rev. B: Condens. Matter Mater. Phys.*, 1981, **23**, 5048–5079.
30 S. Pisana, M. Lazzeri, C. Casiraghi, K. S. Novoselov, A. K. Geim, A. C. Ferrari and F. Mauri, *Nat. Mater.*, 2007, **6**, 198–201.

This journal is © The Royal Society of Chemistry 2014